Russian Journal of Earth Sciences Online ISSN: 1681-1208

Small Lakes Mixing by Surface Cooling: Efficiency Estimates

S. R. Bogdanov[1,*], T. V. Efremova[1], N. I. Palshin[1], and R. E. Zdorovennov[1]

[1]Northern Water Problems Institute of the Karelian Research Centre of the Russian Academy of Sciences, Petrozavodsk, Russian Federation

* **Correspondence to:** Sergey Bogdanov, Sergey.R.Bogdanov@mail.ru

Abstract: The mixing of waterbodies and mixing efficiency estimates for different forcing mechanisms remain one of the main challenges in limnological studies, with a deep theoretical background and a wide range of practical applications. This paper examines the mixing that is triggered by surface cooling during the period of open water. The cooling often occurs at night and is largely determined by infrared radiation fluxes, in this regard, this type of forcing is usually positioned as the radiative mixing mechanism. To calculate the mixing efficiency η, an integral energy method was used, within which this parameter is defined as that portion of the external forcing that is spent on mixing itself, as opposed to viscous dissipation. Specific features of energy fluxes between different energy pools have been revealed for radiative type of forcing. For each identified mixing episode the changes of background potential energy were assessed, together with energy sink due to dissipation. Long-term temperature series for different depths at two small water bodies – a forest lake and a city pond – were used as initial data. Calculations carried out for several hundred mixing episodes showed that the mixing efficiency value, on average, significantly exceeds the canonical threshold 0.17. The correlation has also been identified between efficiency and CML thickness: vertical mixing resistance increases with CML deepening. This result introduces a new challenge to the "universality vs variability" dilemma: the efficiency may depend not only on the type and intensity of forcing, but also on the parameters of the initial temperature profile.

Keywords: mixing efficiency, surface cooling, external forcing, background potential energy, small lakes

Citation: Bogdanov S. R., Efremova T. V., Palshin N. I., and Zdorovennov R. E. (2026), Small Lakes Mixing by Surface Cooling: Efficiency Estimates, *Russian Journal of Earth Sciences*, 26, ES3008, EDN: MMREKA, https://doi.org/10.2205/2026es001090

Review

Received: May 6, 2025
Accepted: November 25, 2025
Published: August 7, 2026

1. Introduction

The problem of mixing of waterbodies remains one of the most challenging in limnological and oceanological research. From a theoretical perspective, this problem represents an important segment of the study of turbulence in a stratified environment. In turn, in practical terms, its significance is determined (but not limited) by the relevance of the related problems such as:

- lakes' classification [*Holgerson et al.*, 2022],
- estimates of gas emission from lake surface [*Rehder et al.*, 2023],
- the development of lake models within the Lake sectors of the global climate simulations (such as, for example ISIMIP [*Golub et al.*, 2022]).

1.1. Methods Overview: Some Theoretical and Experimental Challenges

When studying mixing and its efficiency, as in the case of the more general problem of lake thermal dynamics, a wide range of methods is used, related both to the planning and implementation of experiments, and to modeling. The comprehensive review of the modern trends in water temperature modeling and monitoring approaches are presented, for example, in [*Piccolroaz et al.*, 2024]. The available models, both deterministic and statistical, semi-empirical and computational, range from bulk (0D) to three-dimensional (3D) models with their proper functioning highly dependent on the type and quality of available data. In this article we used a 1D approach, processing data from one thermal chain for each object.

Within the mixing studies, the key issue is the estimation of mixing efficiency η, which determines the fraction of external forcing which is spent on mixing per se, as opposed to viscous dissipation. These estimates may be based on calculations of rates of energy changes in different pools, or correspondent fluxes and turbulent diffusivities, or net changes. As a result, even efficiency definitions and basic notions are not uniquely defined; in the review paper [*Gregg et al.*, 2018], e.g., this multitude is illustrated by the list of definitions, which include more than a dozen items.

In general, the variability of approaches that are currently used in the study of mixing can be characterized and classified by alternatives: dynamic vs energetic, local vs. cumulative. Key parameters used within dynamical approaches are turbulent fluxes and diffusivities. As for energy approaches, one of the first parameters that was used in quantitative assessments of vertical mixing resistance was the Schmidt stability index St [*Idso*, 1973; *Robertson and Imberger*, 1994]. It is defined as the specific (per unit area) work required to mix a stratified column of liquid without heat exchange with the environment (J/m^2):

$$St = \frac{g}{A_s}\int_0^H (z - z_V)\rho(z)A(z)\mathrm{d}z.$$

Here H and z_V are the maximum depth and the center of volume of the lake, A_s – surface area, $\rho(z)$ and $A(z)$ – density and area at depth z, g is acceleration due to gravity. In what follows, we consider the case of the simplest bathymetry, when $A(z) = A_s$.

To assess the efficiency of wind mixing, the dimensionless criteria Wedderburn number and Lake Number L_N related to the St parameter have also become widespread. Expressions for both of these quantities include the dynamic speed u_*, determined by the wind stress on the water surface, and lake fetch length $l \sim \sqrt{A_s}$.

The processing with all three mentioned criteria includes some uncertainty associated with the determination of the threshold values used for distinguishing between mixed and stratified conditions. For example, a value of ~ 5 J/m^2 is used as a threshold for the St parameter [*Guseva et al.*, 2021]; and for parameters W and L_N – values close to 1. This choice should be considered as very conditional, and, accordingly, the description of the stability of the water column using the indicated parameters should be considered primarily as qualitative.

In addition, it should be borne in mind that the dimensionless criteria W and L_N, strictly speaking, cannot serve as time-local parameters characterizing the state of the system. Both of these parameters, in their physical meaning, can be considered as the ratio of two time scales; for example, $L_N \sim \tau_1/\tau_2$, where $\tau_1 = St/(\rho u^{*3})$ is the estimate of the time required for complete mixing at a given wind load, and $\tau_2 = l/u^{*3}$ is "kinematic" time scale. Accordingly, both of these criteria characterize not so much the potential energy itself as the rate of its change under given conditions of external (through the wind) energy pumping.

Further development of the energy approach is usually linked to the works [*Lorenz*, 1955; *Winters et al.*, 1995], in which, in particular, the concepts of background (BPE) and available (APE) potential energies were introduced, by splitting the total potential energy E_p. The value E_b of BPE is defined as the minimum potential energy attainable through an adiabatic redistribution of density towards statically stable sorted profile ρ^*, while the APE value E_a is identified as the potential energy released during such virtual redistribution. Within such approach the efficiency calculation is carried out on the basis of determining the net changes of BPE and APE during irreversible diabatic mixing. Despite all the physical attractiveness of this approach, its specific implementation requires solving a number of specific challenges. The short list of these challenges includes:

- Splitting the energy contribution from different drivers (wind, radiation, wave breaking, precipitation, etc.) [*Guseva et al.*, 2021; *Markfort et al.*, 2010; *Read et al.*, 2012]. For proper estimation of energy net changes in different pools the contribution of each driver should be calculated separately.
- Detailing and clarification of energy paths and energy redistribution between different pools (BPE, kinetic energy KE, internal energy IE, exergy, etc; key energetic parameters used in the text are presented in Table A1 of section A.). Here, the role of IE and its subcomponents in energy path structure remains most challenging [*Tailleux*, 2013].
- The necessity of high-resolution temperature profiles for proper estimation of potential energy, buoyancy fluxes and the energy dissipation rates.
- Distinguishing between mixed (with quasi-homogeneous density structure) and mixing (where turbulent mixing is actively occurring, with high rates of kinetic energy dissipation) layers with depths h_m and h^* [*Brainerd and Gregg*, 1995; *Sutherland et al.*, 2014]. Most estimates of parameters which describe the energy paths are based on the assumption that $h_m = h^*$, but this is often not the case.

As for the quantitative estimates of efficiency η, this problem also remains challenging. The initial assumption about the universality of this value (~ 0.17) for shear-driven turbulence is not supported by numerous experimental data: recent studies proved that η is highly sensitive not only to the type of forcing but also to turbulence parameters [*Bouffard and Wüest*, 2019; *Mashayek et al.*, 2017].

1.2. Problem Statement and Article Structure

In this work, the cumulative energy method is used to calculate the efficiency of the radiative mixing mechanism caused by surface cooling. Cumulative nature of this method includes two aspects – spatial and temporal: net changes of energy in different pools are assessed for the entire water column and during sufficiently long time intervals, for events identified as “mixing episodes”.

The capabilities of this approach were previously analyzed in [*Bogdanov et al.*, 2023]. In particular, one of the fundamental advantages of this approach was noted: the calculation of the energy parameters and the assessment of efficiency can be carried out based on the processing of only temperature experimental data obtained with thermistor chain. The effectiveness of the corresponding techniques is largely determined by the adequate choice of vertical and time discreteness of measurements. Using these techniques, several mixing episodes caused by nighttime cooling during the 2022 summer season were calculated for the small forest lake Golubaya Lamba (GL). When calculating the efficiency η, high values were obtained (~ 0.4), significantly exceeding the canonical estimate of 0.17. Subsequently, the calculations were repeated for a significantly larger (132) number of episodes identified in the 2021 and 2023 seasons [*Bogdanov et al.*, 2024]. The conclusion about abnormally high efficiency values was confirmed.

In addition, a negative correlation was found between the efficiency value and convectively mixed layer (CML) thickness. In this regard, the possible role of density profile shape as a factor causing variability of mixing efficiency was pointed out. This work is a continuation of the above studies, with the special attention to the problem of the universality of efficiency and its possible dependence not only on the type of forcing and turbulence parameters, but also on the state of the water column immediately before mixing.

For the sake of certainty, the consideration is carried out within the framework of the simplest approximation, when the water column can be considered as two-layer, and the profile is approximated by a mixed upper layer of thickness h_m and an underlying stratified one. The task here is to identify the dependence (if any) of the efficiency on the relative thickness h_m/H of the mixed layer.

The results of processing experimental data were also compared with the results of analytical calculations based on the use of a simple model of temperature profile distortion during surface cooling. Within the framework of this model, a direct calculation of the available and background potential energy was carried out.

2. Preprocessing and Methods

2.1. Study Sites

The deep oligotrophic lake GL was selected again as the basic object for studying the radiative mixing mechanism at nights, with special attention to the stage of autumn cooling. The dataset includes temperature measurements from September 6 to October 1, 2023. Thermistor chain included 12 sensors distributed in depth at intervals of 0.5 m (from 0.25 m to 5.75 m), the measurements were carried out with a resolution of 10 minutes.

The study set was complemented by a small shallow (water depth ~ 70 cm) urban pond in the city of Delft (NL). In the following, the designation DP will be used for this object. The experiments on DP were carried out from July 12 to August 7, 2014, temperature monitoring data are presented in the public domain [*Solcerova et al.*, 2019]. The complete mixing of the DP water column was achieved during most nighttime mixing episodes.

For both objects (GL and DP) the surface area (3.9 and 0.36 hectares) and the fetch length (~ 200 m and 60 m) are very small. Following the correlation between area and u_*/w_*, derived in [*Read et al.*, 2012], one can estimate the ratio between velocity scales for wind shear (u_*) and cooling-induced convection (w_*) as 0.25 and 0.025 respectively. It means that cooling is the prevailing mixing mechanism for both sites. It should also be noted that wind-induced mixing is additionally suppressed due to the forested shore of GL and urban environment of DP. Following [*Markfort et al.*, 2010] we estimated sheltering coefficients for both waterbodies and derived the values less than 0.1.

2.2. Identification and Selection of Mixing Episodes

The implementation of the integral energy method is carried out in several sequential steps. The first step was to identify and select mixing episodes. Here various parameters and criteria can be used. In particular, one can explore the parameters directly related to external forcing, for example, the density W (W/m^2) of surface heat flux at night, in the absence of direct solar radiation. Direct calculation of W, however, is complicated by the fact that the value of W includes contributions from long-wave radiation, convection, sensible and latent heat transfer (see, for example, [*Kalinowska*, 2019]). To assess these contributions, additional data on external parameters, including air temperature and humidity, and wind speed, are needed. In the case where data on these parameters are not available, purely internal parameters that describe the lake response to external forcing can be used as an alternative criterion. As such a parameter, one can use (as was accepted in [*Bogdanov et al.*, 2023]) the depth-averaged temperature $\overline{T}$, related to W by the formula (bottom heat fluxes are neglected):

$$\frac{\mathrm{d}\overline{T}}{\mathrm{d}t} = \frac{W}{c\overline{\rho}H}. \tag{1}$$

Here c is the specific heat of water, the bar above the value indicates averaging over the water column. For this case episodes of mixing are identified with time intervals during which the value of $\overline{T}$ decreased. Another alternative criterion can be the BPE which characterizes the transformation of the density profile as a result of external forcing. In this case, the episodes of mixing correspond to periods of BPE growth. In this study we used the "strong" criterion for mixing episodes identification, by applying both requirements. For both objects, calculations were carried out only for intervals during which both criteria were met: the $\overline{T}$ value decreased, and the BPE increased.

In previous papers [*Bogdanov et al.*, 2023, 2024], the mixing study was carried out for GL during the period of summer heating, when the diurnal variations in the thickness of the convective-mixed layer are relatively small and long (~ 12-hours) time intervals, which usually coincided with periods of nighttime cooling, were used as mixing events. This work uses data on the thermal regime of GL obtained during the initial period of autumn cooling, when diurnal variations of h_m value were very large: active restratification during the daytime alternated with a rapid deepening of the lower boundary of the CML during the hours of night cooling. Almost every day there was a change in the thickness of the CML comparable to the thickness of the entire water column. Taking into account the supposed dependence of efficiency on the thickness of the CML, one can expect a significant change in the value of η even in the daily cycle. In this regard, fairly short (10 min) time intervals were used as mixing episodes. In the period from September 8 to 12, 2023, 294 (57+58+72+71+36 respectively) such episodes were identified.

The second object – a pond in Delft – was a significantly less inertial object; complete mixing due to surface cooling occurred practically every summer night ("continuous mixing type", following the terminology suggested in [*Holgerson et al.*, 2022]). In addition, DP pond temperature measurements were made using Distributed Temperature Sensing (DTS) with very high vertical resolution ($\sim$ 0.18 cm), which significantly increased the threshold of sensitivity when calculating changes in BPE. Given these advantages and with the aim of identifying the sensitivity of the result with respect to the choice of episode duration, the efficiency calculation for DP was performed for two alternative definitions of mixing episodes, with a duration of 5 minutes (corresponding to the discreteness of temperature measurements) and 0.5 hours. The number of such episodes was 3240 and 144, respectively.

2.3. Direct Calculations of Net Changes in Different Energy Pools

After mixing episodes identification the changes ΔE_b in the BPE were calculated directly, after proper transformation (adiabatic redistribution towards a gravitationally stable state [*Winters et al.*, 1995]) of temperature and density profiles.

We believe an important novel element in these calculations lies in splitting the potential energy $E_p(t) = g\int_0^{H(t)} \rho(z,t) z \mathrm{d}z$ (and, correspondingly, its variations in time) in two parts: $E_p = E_{p0} + E_p'$. The first part is "inert" potential energy $E_{p0}(t) = g\int_0^{H(t)} \overline{\rho}(t) z \mathrm{d}z = \overline{\rho}(t)H^2(t)/2$; it does not depend on density profile and is governed by mean density $\overline{\rho}$ of the water column. At the same time, variations of both $\overline{\rho}$ and H with time occur mainly due to the heating/cooling of the system and are insensitive to the mixing process. In turn, the second part $E_p'(t) = g\int_0^{H(t)} \rho'(z,t) z \mathrm{d}z$, is directly influenced by molecular mixing process and strongly depends on variations $\rho' = \rho - \overline{\rho}$ of density along vertical. Within 1-D modeling, when the dependence of cross-sectional area on depth is not taken into account, this second part is linearly related to Schmidt stability $St = g\int_0^H (z - z_V)\rho \mathrm{d}z$; $z_V = H/2$ is the center of volume. So, in some sense one can treat this novelty as "Schmidt stability revisited", but having in view that for efficiency estimates just St variations matter, not the value St itself. In this case, during mixing E_p' increases, and St decreases.

The next step includes the calculation of kinetic energy dissipation, which leads to an increase in internal energy E_i. This calculation was carried out within the framework of the assumption of a special type of density profile: the water column during the cooling process was represented by two layers: an upper (CML) of thickness h_m and a bottom stratified layer (see panels *a* and *d* on Figure 1 as illustration). The upper limit of the dissipation rate was estimated by calculation of cumulative (over CML) buoyancy flux $j = \alpha g h_m W/(2c)$ [W/m^2] (α – thermal expansion coefficient) in the CML as described in detail in [*Bogdanov et al.*, 2023]. Then the energy ΔE_i dissipated during mixing event was estimated as $\int j \mathrm{d}t$. The calculation of the integral was carried out by using Equation 1. As a result, for the net change of dissipated energy ΔE_i, the following expression was obtained:

$$\Delta E_i = \frac{\alpha g}{2}\rho H\left(\Delta(h_m\overline{T}) - \int \overline{T}\mathrm{d}h_m\right). \qquad (2)$$

To calculate the CML thickness h_m in Equation 2, different methods can be used [*Sutherland et al.*, 2014], and the results are quite sensitive to their choice. For the GL, such a calculation was carried out using the least squares method, taking into account the shape of the self-similar profile described above; details are presented in [*Bogdanov et al.*, 2024]. For DP, taking into account the high vertical discreteness of temperature measurements, the value of h_m was calculated using the temperature gradient threshold method for the temperature averaged over 50 vertical cells (9 cm). The value of $\sim 1°$C/m ($\sim 0.002°$C difference between adjacent cells) was used as the threshold.

The final step was to calculate the mixing coefficient $\Gamma = \Delta E_b / \Delta E_i$, and, accordingly, efficiency $\eta = \Gamma/(1+\Gamma)$.

2.4. Efficiency Estimates by APE Modeling

Alternatively, we performed the model estimates of the efficiency following the method based on the calculations of the net changes of E_b and the total available mechanical energy E (which include APE E_a and kinetic energy E_k) [*Davies Wykes and Dalziel*, 2014]:

$$\eta = \Delta E_b / \Delta E. \tag{3}$$

Calculations are significantly simplified by choosing such sufficiently long mixing episodes for which in the initial and final states the water column is at rest, so that $\Delta E_k = 0$ and, accordingly, $\Delta E = \Delta E_a$. If, in addition, in the final state the density profile is gravitationally stable, the value of APE in the final state is equal to zero, and the change in this energy parameter is reduced to calculating its value E_{ai} at the initial time. Expression (3) for efficiency then takes the form:

$$\eta = \Delta E_b / E_{ai}. \tag{4}$$

This method, being very demonstrative and simple, at the same time remains not so popular, because in the general case it is not easy to identify and parameterize the final density profile: this profile is well-defined only for a few types of mixing events, e.g., triggered by Rayleigh–Taylor instability [*Davies Wykes and Dalziel*, 2014]. On the other hand, both numerous experiments and numerical simulations results [*Zikanov et al.*, 2002] prove that episodes of overnight cooling in shallow lakes and ponds can be attributed to mixing events of precisely this type. Namely, during such events the initial and final profiles (panels *a* and *d* in Figure 1) can be approximated by two layers: CML and underlying stratified layer, and the mixing leads finally only to an increase of CML thickness and decrease of CML temperature.

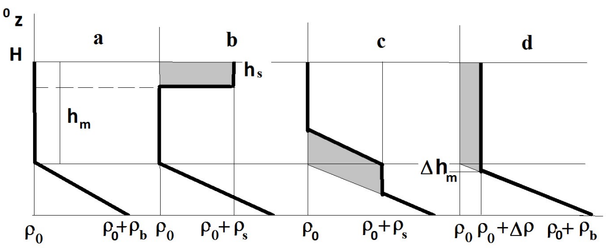

Figure 1. Model profile sequence for mixing event calculations: (*a*) initial, stable; (*b*) initial disturbed, (*c*) initial, after adiabatic sorting, (*d*) final.

Taking this fact into account, the estimates of BPE and APE changes were carried out by using the following self-similar density profile:

$$\rho(z) = \begin{cases} \overline{\rho}, & H - h_m < z < H \\ \rho_b - \dfrac{\rho_b - \overline{\rho}}{H - h_m} z, & z \le H - h_m \end{cases}. \tag{5}$$

Here H is the height of the water column, h_m is CML thickness, ρ_b, $\overline{\rho} = \rho_0 + \Delta\rho$ – density at the bottom and in CML, ρ_0 – reference density.

The energy forcing for each "mixing event" is modeled by the appearance of thin (with thickness h_s) cooled (with density excess ρ_s) layer near surface. For clarity, the sequence of key model profiles (initial, transient/interim, virtual background, final) are present on Figure 1. For such idealized mixing event the efficiency could be calculated directly by applying Equation 4 to initial disturbed and final density profiles presented by panels b and d on Figure 1. The detailed calculations are presented in section B.

3. Results

3.1. General Analysis of Water Temperature Series

The features of the thermal regime of the GL and the nature of mixing during the autumn cooling period are presented in Figure 2, which shows a set of lines describing the temperature changes at different depths. During the period under consideration (from August 22 to October 1), diurnal cycles were clearly observed, within which, in the evening and at night, as a result of cooling, the CML deepened with almost complete mixing of the water column, while during the daytime, under the influence of solar radiation, stratification was restored. The amplitude of daily variations in the surface layers was about 1°C, and the Brent–Väisälä frequency at the moments of maximum stratification reached values of 2×10^{-2} rad/s.

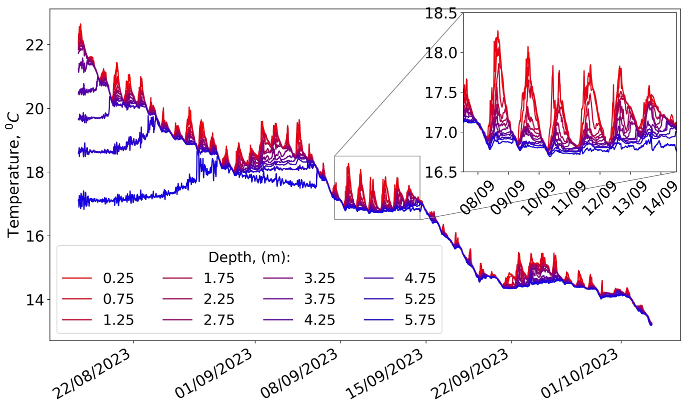

Figure 2. The set of water temperature series for different depths, GL.

Similar results were obtained for DP, in the period from July 9 to 23 (Figure 3). Here the amplitude of oscillations reached 6°C; due to the shallow depth complete mixing was achieved in a shorter time.

The typical daily evolution of temperature profiles for DP is presented in the top panel Figure 4, clearly demonstrating the evening deepening of CML and restratification during daytime. The bottom panel of Figure 4, in turn, illustrates the CML night deepening for GL; almost every night, full mixing of water column was achieved by sunrise.

As stressed in [*Davies Wykes et al.*, 2015; *Tseng and Ferziger*, 2001], the change in the probability density function $f(\rho)$ may serve as the most direct indicator of the diabatic mixing process. To illustrate the issue, calculation of density p.d.f. was carried out according to the formula: $f(\rho) = (H \mathrm{d}\rho/\mathrm{d}z)^{-1}$, after a preliminary adiabatic sorting procedure. The typical daily transformation of this function is presented on Figure 5; the mixing is clearly illustrated by dramatic reduction in dispersion during cooling.

3.2. Changes in Energy Pools Analysis and Efficiency Estimates

The calculations revealed strong correlation between column-averaged temperature decrease and BPE growth, as illustrated by Figure 6. For DP, as a less inert object, the value E_b of BPE reaches the limiting value (corresponding to complete mixing) in a shorter period of time.

The IE and BPE increase during all mixing episodes for each day are nonlinearly connected, as illustrated by curves on correspondent parity diagrams; five such curves for

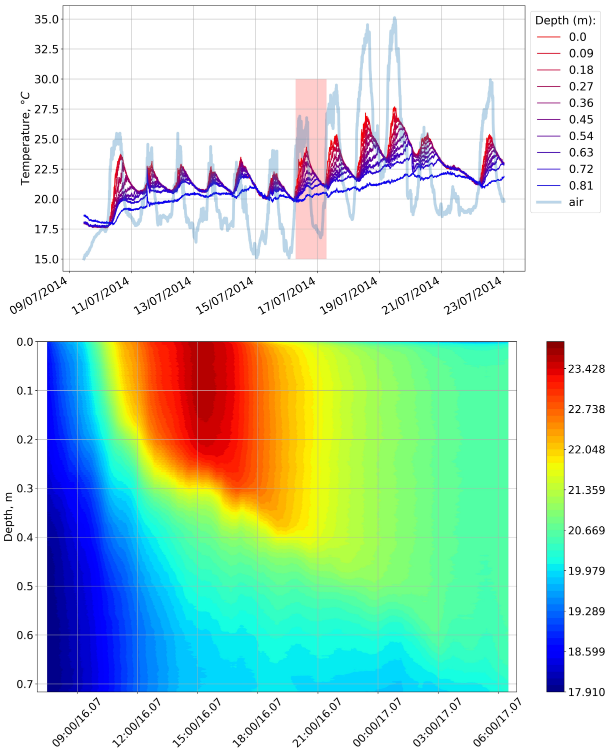

Figure 3. Top panel: water temperature series for different depths, DP. Bottom panel presents the detailed temperature field for the 24-h time interval (from 07:30, July 16, 2014), highlighted on the upper panel.

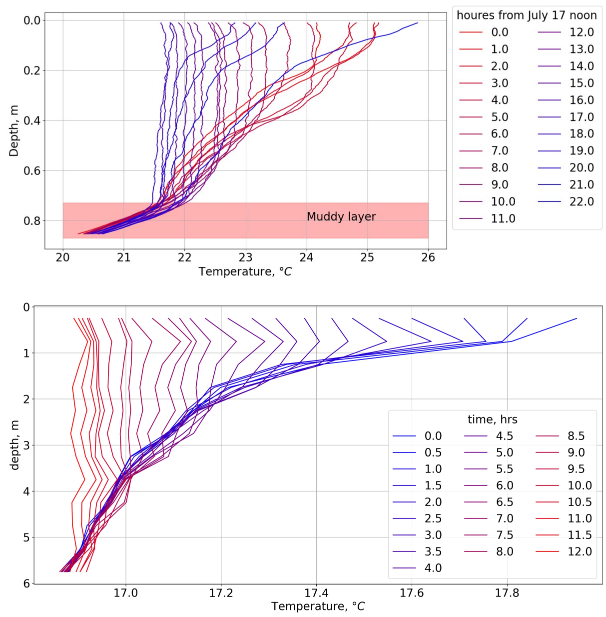

Figure 4. Daily variations of temperature profiles; top panel – DP, July 17, step – 1 hour; bottom panel – GL, September 8, step – 0.5 hours.

GL are presented as an example on the left panel of Figure 7. The concave type of these curves means that the growth rate of BPE slows down during cooling, while the IE growth rate increases. In this regard, it can be assumed that the efficiency of mixing decreases as the CML deepens; this qualitative assumption is quantitatively confirmed by the estimates given below.

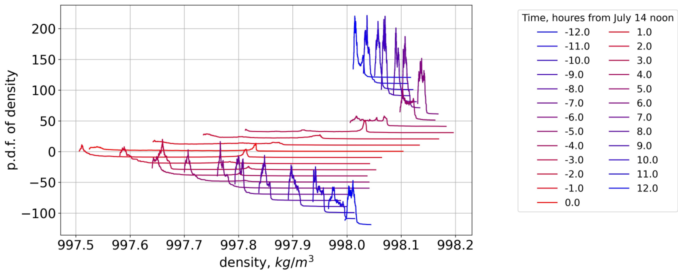

Figure 5. P.d.f. of density, diurnal cycle, July 14, 2014, DP. Each profile is shifted vertically upwards for visualization.

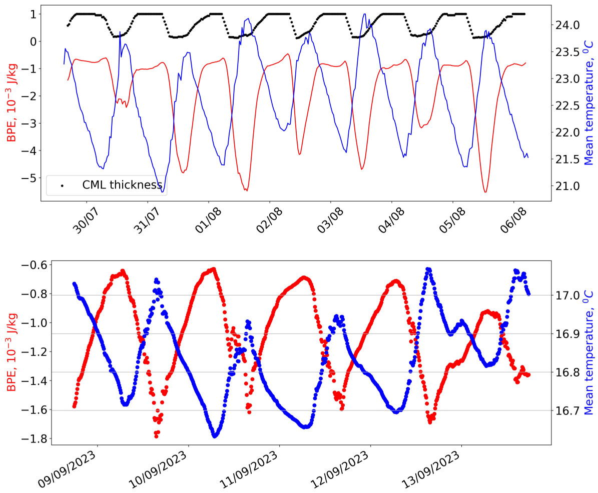

Figure 6. Mean temperature and BPE dynamics; top panel: DP, 2014, bottom panel: GL, 2023.

The results of the efficiency calculations for GL (with a total of 294 episodes) are presented in the right panel of Figure 7. The calculated efficiency values varied over a wide range, and their average values, estimates as ∼ (0.5–0.6), sufficiently exceed the canonical value 0.17. It was also found that the variability of the value of η is associated with its dependence on the thickness h_m of the CML: efficiency monotonically decreases with h_m/H growth. For example, confidence limits fall from (0.54–0.93) to (0.26–0.56) when h_m/H increases from 0.3 to 0.7 (see Figure 7).

Similar results were obtained for DP, for the period from July 20 to August 6. The dependence of η on h_m/H was confirmed by efficiency calculations for both choices of mixing episodes duration (5 min and 30 min), as Figure 8 illustrates.

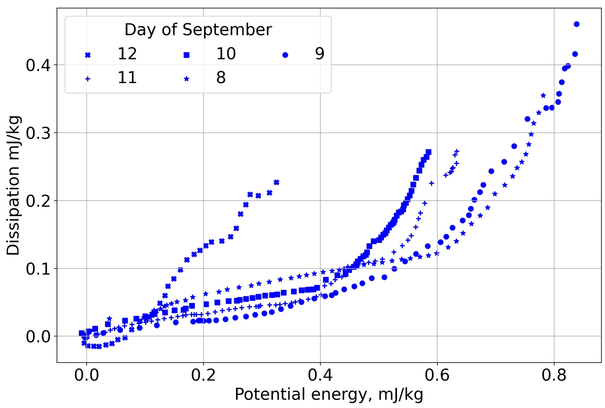

Figure 7. Continued on next page…

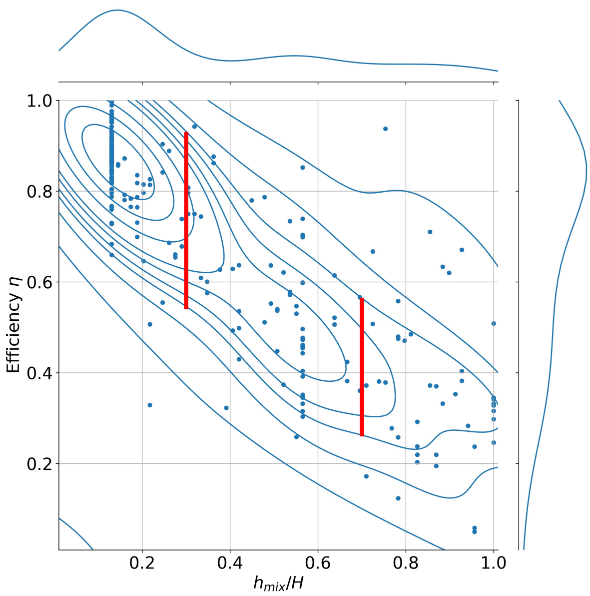

Figure 7. Left panel: BPE and IE growth during mixing episodes for fixed days; GL, from September 8 to 12. Right panel: dependence of mixing efficiency on the relative depth of the mixed layer for GL, September 8–12; markers represent 294 considered 10-min episodes, curves represent both bivariate (10 levels) and univariate graphs of kernel density estimation. Vertical segments correspond to the confidence intervals (for confidence probability 70%) of efficiency for relative depths 0.3 and 0.7.

The conclusion regarding the relationship between η and h_m is also supported at a qualitative level by direct calculations of APE and BPE variations for idealized self-similar density profile (see paragraph below).

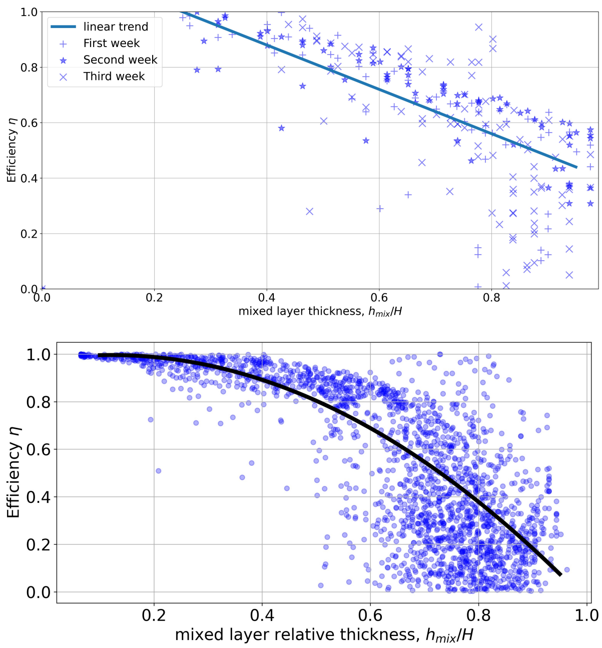

Figure 8. Dependence of mixing efficiency on the relative depth of the mixed layer, DP. Top panel: 0.5-hours mixing episodes (144), bottom panel – 5-min. mixing episodes (3240); the fitting curves are presented by solid lines.

3.3. Model Estimates

The efficiency calculations for the case of an idealized self-similar profile (5) were carried out using Equation 4 for different values of forcing parameters h_s, ρ_s, and bottom density excess ρ_b. The value of $\rho_s \sim \alpha\rho_0\Delta T$ (ρ_0 – reference density) varied within (0.2–2) $\mathrm{kg/m^3}$, corresponding to the excess surface temperature $\Delta T \sim$ (1–10)°C. For relative thickness h_s/H of the disturbed surface layer the values within (0.01–0.1) were used; such highly localized disturbance of density one may regard as the "pulse" profile, previously considered in [*Davies Wykes et al.*, 2015]. Some results of calculations are presented in Figure 9 by the set of lines describing the dependence of mixing efficiency on the relative thickness of the CML when varying the model parameter h_s and the buoyancy frequency $N = \sqrt{g\rho_b/\rho_0/(H-h_m)}$.

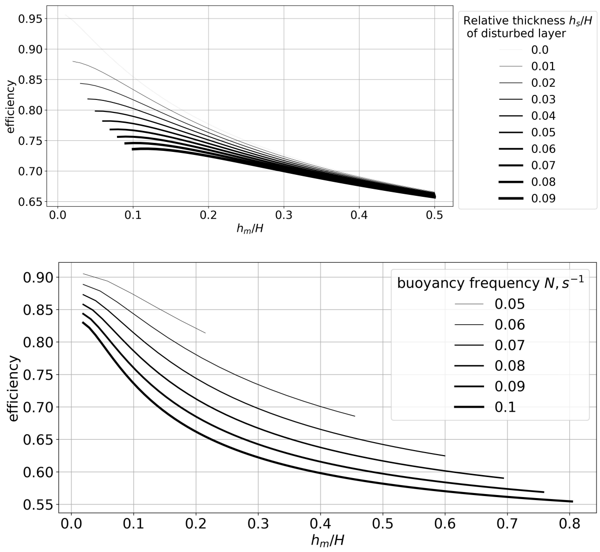

Figure 9. Results of model calculations of efficiency when varying the thickness h_s of the near-surface disturbed layer, with fixed values $\rho_s = 2$ and $N = 0.2$ (top panel) and the buoyancy frequency N in the stratified bottom layer, with fixed values $\rho_s = 0.2$ and $h_s = 0.01$ (bottom panel).

For all acceptable values of the forcing parameters, calculations reveal a monotonically decreasing dependence of the efficiency on the CML relative thickness, from values very close to 1 at small h_m to values close to 0.5 (this last number is usually considered as an asymptotic value of the efficiency for monotonic unstable profiles [*Davies Wykes et al.*, 2015]). These model calculations, carried out for an idealized model, are in qualitative agreement with the result obtained through direct processing of experimental data. It should also be noted that the calculations revealed a significant dependence of the efficiency η on other parameters characterizing both the initial density profile (N) and the forcing (h_s, ρ_s).

4. Discussion and Conclusion

In this work, for the case of radiation forcing associated with surface cooling, values of η were obtained that differ significantly from those accepted for wind mixing. In our view, this difference is expected and associated with the specific features of radiation forcing. The first of these features is that cooling is accompanied by decrease of mean temperature, increase of mean density and, correspondently, by contraction of the water column and decrease of the "inert" potential energy. This decrease matters (it is of the same order as the BPE increase) and should be taken into account during energy flux estimation. The second feature is that the cooling, in contrast to mechanical forcing, triggers changes in the density p.d.f. before mixing per se, as Figure 1a and Figure 1c illustrate.

In general, the results of the analysis indicate that the variability of efficiency may be due not only to its dependence on turbulence parameters noted in many works (see, for example, [*Maffioli et al.*, 2016; *Mashayek et al.*, 2017]), but also on the fact that the value of η may depend on the parameters characterizing the initial density profile. In particular, a negative correlation between η and CML thickness was revealed. In a certain sense, this means that thermal resistivity increases with CML thickening, and the mixing of the bottom stratified layer slows down. This result, if confirmed by further research, is of particular interest in the context of the Cold Bottom problem, which is actively discussed in the literature [*Pilla et al.*, 2020]. Its essence lies in the fact that, under the influence of climate change, the surface temperature of inland water bodies increases, but in the bottom layers this trend is much less pronounced.

Physically, the nature of the dependence of η on h_m is not yet entirely clear. However, this finding is consistent with the previously formulated suggestion [*Davies Wykes et al.*, 2015] concerning the role of remote zones in mixing energetics. Namely, it was supposed that for some unstable initial profiles the special energy path – direct conversion of APE into BPE – become possible due to the presence of regions that initially contribute to APE, but are not in fact involved in the turbulent flow and do not undergo any physical mixing. For the idealized profile presented in Figure 1, the role of such a region is played by that part of the bottom stratified layer in which the density varies in the range $[\rho_0 + \Delta\rho, \rho_0 + \rho_s]$.

In further studies, we plan to verify the conclusion about the dependence of mixing efficiency on the shape of the initial profile, and clarify profile parameters that determine this dependence. In this regard it is planned to use more sophisticated models of profile, taking into account such features as the presence of entrainment layer, nonlinear dependence of temperature on depth, and even the distinction between mixed and mixing layers due to thermal inertia. The last feature is especially significant, since dissipation is assessed using Equation 3, which includes the thickness h_m.

Thermal inertia should also be taken into account during mixing episodes identification, because the profile adjustment occurs with a delay in relation to the external forcing, and the wrong choice of duration τ of episodes can lead to distorted efficiency estimates. In the present paper, the choice of τ was made by taking into account the vertical profile model (two-layer, CML + bottom stratified layer) adopted in the work. For such profiles the value τ can be identified with the relaxation time ("lifetime") τ_r of energy-containing eddies. The size of such eddies is usually identified with the thickness h_m of the CML, and the characteristic velocity w_* is determined by the surface buoyancy flux j: $w^* = (jh_m)^{1/3} \sim (\epsilon h_m)^{1/3}$. Accordingly, characteristic "lifetime" of the eddies can be estimated as $(h_m^2/\epsilon)^{1/3}$. Taking into account the values of $h_m \sim 1$ m and $\epsilon \sim (10^{-8}$–$10^{-7})$ m^2/s^3 characteristic of the objects considered in the article, we obtain a numerical estimate for τ_r of $\sim$ (500–2500) s, or $\sim$ (8–40) minutes. The episodes considered in the article (with duration 10 min for GL and 5 min and 0.5 hours for DP) are close in duration to the calculated limiting values. In the general case, however, the problem of identifying mixing episodes and the choosing of their duration remains challenging.

Acknowledgments. This research was supported by the federal budget within the framework of the state assignment FMEN-2026-0011 "Functioning of the ecosystem of Lake Onega and lake-river systems of its catchment area under conditions of climate change and anthropogenic impact". The authors would like to thank G. E. Zdorovennova for helpful discussions and important comments.

Appendix A. Energy Pools and Fluxes

Table A1. Key energetic parameters used in the text.

Variable name/ abbreviation	Mathematical symbol	Units
Potential energy	$E_p(t) = g\int_0^{H(T)} \rho(z,t)z\mathrm{d}z$	J/m^2
Background potential energy / BPE	$E_b(t) = g\int_0^{H(T)} \rho^*(z,t)z\mathrm{d}z$	J/m^2
Available potential energy / APE	$E_a = E_p - E_b$	J/m^2
Internal energy / IE	E_i	J/m^2
"Inert" potential energy	$E_{p0}(t) = g\int_0^{H(T)} \overline{\rho}(z,t)z\mathrm{d}z$	J/m^2
Mixing-sensitive part of potential energy	$E'_p = E_p - E_{p0}$	J/m^2
Total available mechanical energy	E	J/m^2
The density of surface heat flux at night	W	W/m^2
Cumulative buoyancy flux	$j = \alpha g h_m W/(2c)$	W/m^2

Appendix B. Calculations of APE and BPE Changes for Idealized Self-Similar Profile

The calculation of the potential energies E_{pi}, E_{bi} and E_{pf}, respectively, in the initial disturbed state b, in the virtual state c (after adiabatic reordering to a gravitationally stable state), and also in the final state d (Figure 1) is carried out directly using the formula $E_p(t) = g\int_0^{H(T)} \rho(z,t)z\mathrm{d}z$:

$$\begin{aligned}
E_{pi} &= \rho_s h_s(H - h_s/2) + \rho_b^3 a^2/6,\\
E_{bi} &= \rho_s((\rho_b - \rho_s)a + h_s)^2/2 + (\rho_b - \rho_s)^3 a^2/6 + a\rho_s^2((\rho_b - \rho_s)a + h_s + a\rho_s/3)/2,\\
E_{pf} &= H^2\Delta\rho/2 + a^2(\rho_b - \Delta\rho)^3/6.
\end{aligned}$$

Here $a \equiv g/(\rho_0 N^2)$, $\Delta\rho$ – change in density in the mixed layer that occurred during the current mixing episode (transition from state b to state d). The change in volume during mixing episode can be neglected as a small value in terms of the parameters $\alpha gH/c$ and ρ_b/ρ_0, which makes it possible to directly calculate the value of $\Delta\rho$ from the condition of constant volume:

$$\Delta\rho = \left(\sqrt{h_m^2 + 2ah_s\rho_s} - h_m\right)/a$$

The mixing episodes were chosen in such a way that the profile in the final state d was gravitationally stable; for such states the available potential energy is 0 and, accordingly, $E_{bf} = E_{pf}$. As a consequence, the BPE increment was calculated using the formula $\Delta E_b \equiv E_{pf} - E_{bi}$. In turn, the available potential energy was identified with the APE value in the initial state: $E_{ai} \equiv E_{pi} - E_{bi}$.

References

Bogdanov S. R., Palshin N. I., Zdorovennov R. E., et al. Estimation of mixing efficiency of a small dimictic lake due to surface cooling // Fundamental and Applied Hydrophysics. — 2023. — Vol. 16, no. 2. — P. 73–88. — https://doi.org/10.59887/2073-6673.2023.16(2)-6 — (In Russian).

Bogdanov S. R., Zdorovennova G. E., Zdorovennov R. E., et al. Features of mixing the water mass of a small lake during night cooling // Proceedings of the Karelian Research Centre of the Russian Academy of Sciences. — 2024. — No. 2. — P. 25–38. — https://doi.org/10.17076/lim1874 — (In Russian).

Bouffard D. and Wüest A. Convection in Lakes // Annual Review of Fluid Mechanics. — 2019. — Vol. 51, no. 1. — P. 189–215. — https://doi.org/10.1146/annurev-fluid-010518-040506

Brainerd K. E. and Gregg M. C. Surface mixed and mixing layer depths // Deep Sea Research Part I: Oceanographic Research Papers. — 1995. — Vol. 42, no. 9. — P. 1521–1543. — https://doi.org/10.1016/0967-0637(95)00068-h

Davies Wykes M. S. and Dalziel S. B. Efficient mixing in stratified flows: experimental study of a Rayleigh-Taylor unstable interface within an otherwise stable stratification // Journal of Fluid Mechanics. — 2014. — Vol. 756. — P. 1027–1057. — https://doi.org/10.1017/jfm.2014.308

Davies Wykes M. S., Hughes G. O. and Dalziel S. B. On the meaning of mixing efficiency for buoyancy-driven mixing in stratified turbulent flows // Journal of Fluid Mechanics. — 2015. — Vol. 781. — P. 261–275. — https://doi.org/10.1017/jfm.2015.462

Golub M., Thiery W., Marcé R., et al. A framework for ensemble modelling of climate change impacts on lakes worldwide: the ISIMIP Lake Sector // Geoscientific Model Development. — 2022. — Vol. 15, no. 11. — P. 4597–4623. — https://doi.org/10.5194/gmd-15-4597-2022

Gregg M. C., D'Asaro E. A., Riley J. J., et al. Mixing Efficiency in the Ocean // Annual Review of Marine Science. — 2018. — Vol. 10, no. 1. — P. 443–473. — https://doi.org/10.1146/annurev-marine-121916-063643

Guseva S., Casper P., Sachs T., et al. Energy Flux Paths in Lakes and Reservoirs // Water. — 2021. — Vol. 13, no. 22. — P. 3270. — https://doi.org/10.3390/w13223270

Holgerson M. A., Richardson D. C., Roith J., et al. Classifying Mixing Regimes in Ponds and Shallow Lakes // Water Resources Research. — 2022. — Vol. 58, no. 7. — e2022WR032522. — https://doi.org/10.1029/2022wr032522

Idso S. B. On the concept of lake stability // Limnology and Oceanography. — 1973. — Vol. 18, no. 4. — P. 681–683. — https://doi.org/10.4319/lo.1973.18.4.0681

Kalinowska M. B. Effect of water-air heat transfer on the spread of thermal pollution in rivers // Acta Geophysica. — 2019. — Vol. 67, no. 2. — P. 597–619. — https://doi.org/10.1007/s11600-019-00252-y

Lorenz E. N. Available Potential Energy and the Maintenance of the General Circulation // Tellus. — 1955. — Vol. 7, no. 2. — P. 157–167. — https://doi.org/10.1111/j.2153-3490.1955.tb01148.x

Maffioli A., Brethouwer G. and Lindborg E. Mixing efficiency in stratified turbulence // Journal of Fluid Mechanics. — 2016. — Vol. 794. — R3. — https://doi.org/10.1017/jfm.2016.206

Markfort C. D., Perez A. L. S., Thill J. W., et al. Wind sheltering of a lake by a tree canopy or bluff topography // Water Resources Research. — 2010. — Vol. 46, no. 3. — W03530. — https://doi.org/10.1029/2009wr007759

Mashayek A., Salehipour H., Bouffard D., et al. Efficiency of turbulent mixing in the abyssal ocean circulation // Geophysical Research Letters. — 2017. — Vol. 44, no. 12. — P. 6296–6306. — https://doi.org/10.1002/2016gl072452

Piccolroaz S., Zhu S., Ladwig R., et al. Lake Water Temperature Modeling in an Era of Climate Change: Data Sources, Models, and Future Prospects // Reviews of Geophysics. — 2024. — Vol. 62, no. 1. — e2023RG000816. — https://doi.org/10.1029/2023rg000816

Pilla R. M., Williamson C. E., Adamovich B. V., et al. Deeper waters are changing less consistently than surface waters in a global analysis of 102 lakes // Scientific Reports. — 2020. — Vol. 10, no. 1. — P. 20514. — https://doi.org/10.1038/s41598-020-76873-x

Read J. S., Hamilton D. P., Desai A. R., et al. Lake-ize dependency of wind shear and convection as controls on gas exchange // Geophysical Research Letters. — 2012. — Vol. 39, no. 9. — P. L09405. — https://doi.org/10.1029/2012gl051886

Rehder Z., Kleinen T., Kutzbach L., et al. Simulated methane emissions from Arctic ponds are highly sensitive to warming // Biogeosciences. — 2023. — Vol. 20, no. 14. — P. 2837–2855. — https://doi.org/10.5194/bg-20-2837-2023

Robertson D. M. and Imberger J. Lake Number, a Quantitative Indicator of Mixing Used to Estimate Changes in Dissolved Oxygen // Internationale Revue der gesamten Hydrobiologie und Hydrographie. — 1994. — Vol. 79, no. 2. — P. 159–176. — https://doi.org/10.1002/iroh.19940790202

Solcerova A., Ven F. van de and Giesen N. van de. Nighttime Cooling of an Urban Pond // Frontiers in Earth Science. — 2019. — Vol. 7. — P. 156. — https://doi.org/10.3389/feart.2019.00156

Sutherland G., Reverdin G., Marié L., et al. Mixed and mixing layer depths in the ocean surface boundary layer under conditions of diurnal stratification // Geophysical Research Letters. — 2014. — Vol. 41, no. 23. — P. 8469–8476. — https://doi.org/10.1002/2014gl061939

Tailleux R. Available Potential Energy and Exergy in Stratified Fluids // Annual Review of Fluid Mechanics. — 2013. — Vol. 45, no. 1. — P. 35–58. — https://doi.org/10.1146/annurev-fluid-011212-140620

Tseng Y.-h. and Ferziger J. H. Mixing and available potential energy in stratified flows // Physics of Fluids. — 2001. — Vol. 13, no. 5. — P. 1281–1293. — https://doi.org/10.1063/1.1358307

Winters K., Lombard P., Riley J., et al. Available potential energy and mixing in density-stratified fluids // Journal of Fluid Mechanics. — 1995. — Vol. 289. — P. 115–128. — https://doi.org/10.1017/s002211209500125x

Zikanov O., Slinn D. and Dhanak M. Turbulent convection driven by surface cooling in shallow water // Journal of Fluid Mechanics. — 2002. — Vol. 464. — P. 81–111. — https://doi.org/10.1017/s0022112002001015